BIOCHEMICAL AND BIOPHYSICAL RESEARCH COMMUNICATIONS **231,** 126–130 (1997)
ARTICLE NO. RC976059

Precise Limits of the N-Terminal Domain of DnaB Helicase Determined by NMR Spectroscopy

Caroline S. Miles,* Johan Weigelt,† N. Patrick J. Stamford,* Nada Dammerova,* Gottfried Otting,†,[1] and Nicholas E. Dixon*,[2]

**Centre for Molecular Structure and Function, Research School of Chemistry, Australian National University, Canberra, ACT 0200, Australia; and †Department of Medical Biochemistry and Biophysics, Karolinska Institute, S-171 77 Stockholm, Sweden*

Received December 17, 1996

Two separate N-terminal fragments of the 470-amino-acid *Escherichia coli* DnaB helicase, comprising residues 1-142 and 1-161, were expressed in *E. coli.* The proteins were extracted in a soluble fraction, purified, and characterised physically. In contrast to the full-length protein, which is hexameric, both fragments exist as monomers in solution, as demonstrated by sedimentation equilibrium measurements. CD spectroscopy was used to confirm that the 161-residue fragment is highly structured (mostly α-helical) and undergoes reversible thermal denaturation. The structurally well-defined core of the N-terminal domain of the DnaB helicase is composed of residues 24 to 136, as determined by assignment of resonances from flexible residues in NMR spectra. The ^{1}H NMR signals of the flexible residues are located at random coil chemical shifts, and their linewidths are significantly narrower than those of the structured core, indicating complete disorder and increased mobility on the nanosecond time scale. The results support the idea of a flexible hinge region between the N- and C-terminal domains of the native hexameric DnaB protein.

DnaB, a hexamer of subunits of molecular weight 52,265 (1-3), is one of the key proteins in *Escherichia coli* chromosomal replication, playing an important role during both the initiation and elongation stages. As well as interacting with other replication proteins, it binds to both single- and double-stranded DNAs, rNTPs and dNTPs, and exhibits DNA-dependent rNTPase activity (1). During replication initiation, DnaB is loaded onto single-stranded DNA through interactions with both the DnaA and DnaC proteins (4-6). At the elongation stage, DnaB fulfils its role as the major replicative DNA helicase, using the energy it obtains through ATP hydrolysis to unwind the DNA duplex to generate single-stranded DNA (7). Once the DNA strands have been separated, the synthesis of short RNA primers by the DnaG primase ensues to allow lagging strand replication by DNA polymerase III holoenzyme (8).

A high-resolution structure of DnaB is essential for full understanding of its reaction mechanisms, and the work described here is a first step in that direction. We previously proposed a structural model (9) based on a reconstruction of electron microscopic images of negatively-stained DnaB in the presence of ATP. The model, representing the protein at a medium resolution of 2.7 nm, shows it to be triangular in shape, consisting of a trimer of dimers with a 4-nm diameter channel through the center of the molecule. The features of this model are consistent with the conclusions of Nakayama *et al.* (3) who, following studies of trypsin hydrolysis, proposed each subunit of 470 amino acid residues to be composed of two distinct structural domains. More recent electron microscopic studies using a variety of nucleotide cofactors, including ATP, show that in addition to rings with 3-fold symmetry as found previously, rings with 6-fold symmetry are observed, as well as some in an intermediate state (10). This indicates that there may be an equilibrium between two different conformations of the hexameric ring, where three of the subunits remain more or less fixed, and the other three, or one of their domains, undergo a large rotation.

The work detailed in this paper concerns the N-terminal domain of the DnaB helicase. The ~12-kDa N-terminal tryptic fragment has been shown to be essential for helicase activity (3,11) and interactions with other proteins (3) and appears to exert a strong influence on hexamer formation (11). The 33-kDa C-terminal domain contains the sites for DNA and ATP binding (3,11) and alone can only form stable dimers (11). Based on the proteolytic studies and secondary struc-

[1] Corresponding author. Fax: 46 (8) 335296. E-mail: go@mfn.ki.se.
[2] Corresponding author. Fax: 61 (6) 2490750. E-mail: dixon@rsc.anu.edu.au.

0006-291X/97 $25.00

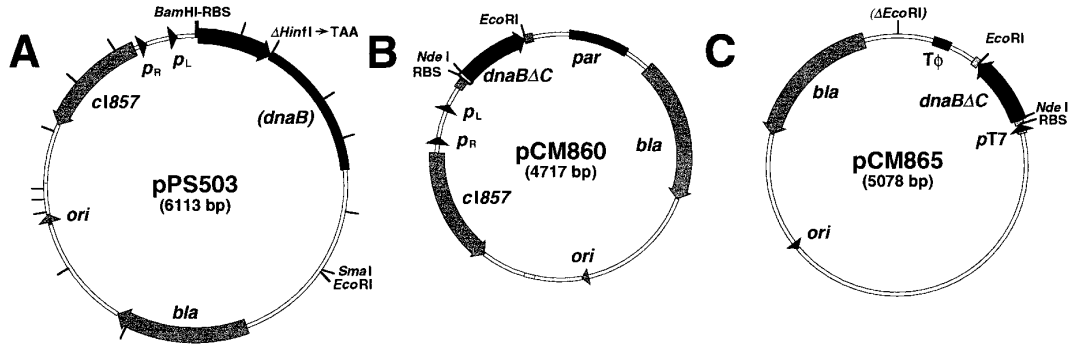

FIG. 1. Physical maps of plasmids that directed overproduction of the N-terminal domain of the DnaB helicase. (A) pPS503 [DnaBΔC(162-470)] was constructed by duplication of the overhanging ends of the identified *Hin*fI restriction site in the *dnaB*$^+$ plasmid pPS359 (13). The remaining 12 *Hin*fI sites in pPS503 are marked. This creates an in-frame TAA (stop) codon after the Glu 161 codon of *dnaB*. The plasmid pPS359, which directs transcription of *dnaB* from λ promoters and a synthetic RBS, had been constructed by BAL 31-treatment of a *Hpa*I-linearised *dnaB*$^+$ derivative of pPT150 as described (14). (B) pCM860 [DnaBΔC(143-470)] was constructed by insertion of a PCR-generated *Nde*I-*Eco*RI fragment between corresponding sites in the λ-promoter vector pND706 (15). (C) pCM865 [DnaBΔC(143-470)] was constructed by insertion of the same *Nde*I-*Eco*RI fragment into the T7-promoter vector pETMCSI, a derivative of pET3c (16).

ture predictions, it was suggested that DnaB consists of a hydrophilic 20-residue N-terminal region followed by an N-terminal domain (residues 21-127) with mainly α-helical secondary structure (3,12). Residues 173-470 were suggested to form a larger, flexible domain. It was considered that the region between the two domains could be a hinge.

Our aim was to define unambiguously with experimental data the precise boundaries of the structurally rigid part of the N-terminal domain fragment DnaBΔC-(162-470) (comprising residues 1-161) and to probe the existence of a flexible hinge between the two domains. The approach taken was to use NMR spectroscopy to assign the ^{1}H NMR resonances of the highly mobile amino acid residues of the fragment. Although there are NMR experiments where the signals from mobile residues can be observed selectively, their signals tend to overlap badly. As it is not always possible, therefore, to assign the resonances of segments with more than about 20 residues in random coil conformation from homonuclear ^{1}H NMR spectra, a 142-residue fragment, DnaBΔC(143-470), was also used in the study.

MATERIALS AND METHODS

Construction of plasmid pPS503 for the overexpression of DnaBΔC-(162-470). Plasmid pPS503 was constructed from pPS359 (13), a derivative of pPT150 (14) which contains the *dnaB* gene (Fig. 1A). pPS359 was partially digested with *Hin*fI restriction endonuclease and full-length, linearised, plasmid DNA was isolated from an agarose gel. The ends were filled using the Klenow fragment of DNA polymerase I and the plasmid recircularised. After transformation of *E. coli* AN1459, ampicillin-resistant transformants were selected at 30 °C. Plasmid DNAs of the required size (6113 bp) were then screened by comparison of *Hin*fI fragment patterns on agarose gels with those from *Hin*fI-digested pPS359. Those plasmids missing the second of the four *Hin*fI sites within *dnaB* were selected and analysed for the expression of an N-terminal fragment of DnaB protein at 42 °C, as visualised on SDS-PAGE. Among those isolated was one that promoted overproduction of the DnaBΔC(162-470) fragment, formed by the generation of a TAA stop codon immediately after the Glu 161 codon.

Generation of DnaBΔC(143-470). This deletion mutant of *dnaB* was generated using a PCR strategy with pPS503 as template. Two primers were designed: the first (5′-CCGGGAGCTCGAATTCTT-AGGCAATCTCATTCGCAACC) to insert a TAA stop codon followed by an *Eco*RI restriction site immediately after the Ala 142 codon of *dnaB;* the second (5′-GAAGGAGATATACATATGGCAGGAAATAAA-CCCTTC) to generate an *Nde*I restriction site at the ATG start codon. The PCR reaction mixture (50 μL) contained template plasmid pPS503 (77 pg), both primers (1 μM of each), $MgSO_4$ (1 mM), all four dNTPs (1 μM of each), Vent DNA Polymerase (1 unit, New England Biolabs) and NE Buffer for Vent DNA Polymerase (New England Biolabs). The thermal cycler was programmed as follows: 94 °C for 5 min; 94 °C for 15 s, 55 °C for 15 s and 72 °C for 45 s (3 times); 94 °C for 15 s, 72 °C for 15 s and 72 °C for 45 s (32 times); 20 min at 72 °C and 5 min at 25 °C. The amplified DNA (463 bp) was purified using Wizard PCR Preps (Promega) and digested with *Nde*I and *Eco*RI. The fragment was ligated to the 4282-bp *Nde*I-*Eco*RI fragment of pND706 (15). Ampicillin-resistant transformants of AN1459 were selected at 30 °C and plasmid DNAs were isolated on a small scale (expected size 4717 bp). Overproduction of the desired 15.7-kDa protein at 42 °C was confirmed by SDS-PAGE. The sequence of *dnaBΔC(143-470)* from the selected plasmid, pCM860 (Fig. 1B), was confirmed by amplification of the DNA using an ABI PRISM dye terminator cycle sequencing kit and subsequent analysis using an Applied Biosystems 373A sequencer.

Construction of plasmid pCM865 for the overexpression of DnaBΔC-(143-470). Plasmid pCM865 (Fig. 1C) was constructed by insertion, between the *Nde*I and *Eco*RI sites of pETMCSI, of *dnaBΔC(143-470)* excised from pCM860 on a 435-bp *Nde*I-*Eco*RI fragment. pETMCSI is a derivative of the pET vectors described by Studier *et al.* (16), relying on transcription from the phage T7 φ10 promoter. The *Eco*RI site at the sequence origin of pBR322 in the pET3c vector was removed so that the *Eco*RI site in the polylinker region, which is similar to that found in pND706 (15), is unique. pETMCSI contains an *Nde*I site downstream of the φ10 RBS (Fig. 1C) and can be used to provide a new, strong RBS. Ampicillin-resistant transformants of *E. coli* BL21(DE3) were selected at 37 °C. Plasmid DNAs were isolated on a small scale and their sizes verified on 0.7% agarose gels (5078 bp). Overproduction of the 15.7-kDa protein following IPTG induction (0.5 mM) at 37 °C was checked by SDS-PAGE.

Bacterial growth. *E. coli* strains were grown in 6 × 1 L LB medium supplemented with 25 μg/mL thymine and 50 μg/mL ampicillin. Strain AN1459/pPS503 was grown at 30 °C until A_{595} = 0.5 then heated rapidly to and incubated for 4 h at 42 °C. Strain BL21(DE3)/pCM865 was grown at 37 °C until A_{595} = 0.5. Protein production was induced by the addition of 0.5 mM IPTG and cultures were grown for 2 h at the same temperature. Cells were harvested by centrifugation, yielding 3.6-4 g/L of culture.

Protein extraction. Cells were resuspended in lysis buffer (50 mM Tris.HCl pH 7.6, 10% w/v sucrose, 200 mM NaCl, 10 mM spermidine-Cl; 15 mL/g cells). Lysozyme (chicken egg white, Sigma) was added to 0.25 mg/mL and the suspension was stirred at 4 °C for 2 h before being heated at 37 °C for 4 min. After treatment at 4 °C for a further 30 min, the lysate was centrifuged (38,700 × *g*, 30 min, 4 °C). The supernatant was set aside at 4 °C. The pellet was resuspended in the original volume of lysis buffer, passed through a French Press (12 kpsi) and centrifuged. The supernatants were mixed and ammonium sulphate (0.27 g/mL) was added over a period of 1 h. The solution was left to stir under the same conditions for a further hour before being centrifuged (38,700 × *g*, 45 min, 4 °C). The supernatant was discarded and the pellet was resuspended in the minimum volume of Buffer A (50 mM Tris.HCl pH 7.6, 20% glycerol, 5 mM $MgCl_2$). The solution (Fraction I) was dialysed overnight at 4 °C against two changes of Buffer A.

Protein purification and concentration. The two DnaB deletion mutant proteins were further purified at 4 °C using anion-exchange chromatography and gel-filtration. Fraction I was clarified by centrifugation and loaded at a flow rate of 0.8 mL/min onto a column (70 mL) of DEAE-Fractogel (Merck) equilibrated in Buffer A. After washing with two column volumes of Buffer A, a linear gradient of NaCl in Buffer A was applied (0.01 M increase/25 min). The required proteins were eluted between 0.07 and 0.15 M NaCl. The purest fractions, as determined by SDS-PAGE, were pooled and precipitated with ammonium sulphate (0.315 g/mL). The pellets were resuspended in a maximum of 5 mL of Buffer C (50 mM Tris.HCl pH 7.6, 15% glycerol, 100 mM NaCl, 5 mM $MgCl_2$) and loaded onto a Sephadex G-50 gel-filtration column (250 mL, Pharmacia), equilibrated in Buffer C, at a flow rate of 0.5 mL/min. Protein fractions of >95% purity (as determined by SDS-PAGE) were pooled and dialysed against Buffer D [10 mM Tris.HCl pH 7.6, 20 mM NaCl, 5 mM $MgCl_2$; for DnaBΔC(162-470)] or E [20 mM potassium phosphate pH 7.0; for DnaBΔC(143-470)]. Proteins were concentrated using a vacuum dialysis apparatus (Schleicher & Schuell) and their concentrations were determined by the Bradford method using BSA as standard (17). Further concentration of the proteins for preparation of NMR samples was carried out using an ultrafiltration cell with YM10 membranes (Amicon).

Protein characterisation. For analysis by electrospray mass spectrometry, protein samples (0.5-1 mg) were diluted to 1 mL in milli-Q water and dialysed extensively against 0.1% formic acid. Samples were run on a VG Quattro II mass spectrometer (VG Biotech Ltd) equipped with an electrospray ionisation source and a quadrupole-hexapole-quadrupole mass analyser. All spectra were analysed using software supplied by the manufacturer.

Protein samples for N-terminal sequence analysis (1 pmol) were prepared as described above and analysed on an Applied Biosystems Procise Sequencer. Twelve cycles were acquired at a sampling rate of 4 Hz.

Sedimentation equilibrium studies were carried out using a Beckman Optima XL-A analytical ultracentrifuge (25 °C, 25 krpm). Double-sector cells of 12-mm path-length were used, with the protein sample (100 μL) in one compartment and the corresponding buffer (110 μL, Buffers D or E) in the other. Data were analysed using programs XLAEQ and XLAMW (Beckman) assuming ρ = 1.00 g/mL and $\bar{\nu}$ = 0.73 mL/g.

CD spectroscopy was performed with samples of 0.15 mg/mL DnaBΔC(162-470) in 20 mM sodium phosphate, at pH values ranging from 3.5 to 7.5. Spectra were recorded in the wavelength interval 195-260 nm at 25 °C on an AVIV 62DS circular dichroism spectrometer, using a slitwidth of 1.5 nm, a stepsize of 0.5 nm and a 1 s time constant. A sample at pH 6.6 was used to record spectra in the temperature range 15-50 °C, and a melting curve at 220 nm. The melting curve was recorded, using a slitwidth of 3 nm and a 5 s time constant, between 25 and 70 °C by increasing the temperature at a rate of 0.5 °C/min. A 1-mm quartz cuvette was used for all measurements.

NMR spectroscopy. NMR measurements were performed at 28 °C with protein solutions of approximately 1.8 mM in 90% H_2O/10% D_2O containing 20 mM sodium phosphate buffer, at pH 6.2 and pH 6.7 for DnaBΔC(162-470) and DnaBΔC(143-470), respectively. 2D ^{1}H NMR experiments were carried out at 600 MHz on a Bruker DMX-600 NMR spectrometer. TOCSY (18) experiments with a 100-ms mixing time were recorded to identify the spin systems of the mobile residues. ROESY (19,20) experiments were performed with a 100-ms mixing time to observe sequential connectivities between the residues. Besides conventional ROESY, F_1-decoupled ROESY (21,22) and F_1,F_2-doubly-decoupled ROESY (23) experiments were recorded. An F_1,F_2-doubly-decoupled TOCSY (18,21-23) spectrum of DnaBΔC(143-470) was recorded to measure the line-widths of the amide proton signals. Decoupling in F_1 was achieved by the combination of a semi-selective 180° REBURP pulse (24) applied to the α-protons and a non-selective 180° pulse in the center of the t_1 evolution time, which effectively decouples the α-proton resonances from the amide and β-protons (21,22). Decoupling of the amide protons in the F_2 dimension of the F_1,F_2-doubly-decoupled experiments was achieved by SESAM decoupling (23,25) applied to the α-protons using a train of semi-selective hyperbolic secant pulses (26) with the MLEV-16 supercycle (27). Mixing times of 100 ms were found to be sufficient for nearly complete suppression of the signals from the structured parts of the fragments while the more slowly relaxing signals from the unstructured ends were obtained with little attenuation. Solvent suppression was performed by presaturation of the water resonance prior to the first excitation pulse. The Fourier transformed data sets were baseline corrected using the algorithm of Friedrichs (28). All processing was performed using the software program PROSA (29). The TOCSY spectra of DnaBΔC(162-470) and DnaBΔC(143-470) shown in Fig. 2 were recorded with t_1^{max} = 108 and 92 ms and t_2^{max} = 141 and 225 ms, respectively. The total experimental times were 10 and 5 h, respectively.

RESULTS AND DISCUSSION

Good yields of soluble protein were obtained from the two expression systems used (up to 56 mg of pure protein/L culture). As the initiator methionine residue of DnaB protein is cleaved *in vivo* (12), the N-terminal sequences of the two DnaB deletion mutants were analysed (12 cycles), confirming the absence of this residue in both cases. The sequences were otherwise as predicted from the published nucleotide sequence (12). Electrospray mass spectrometry was used to determine accurately the molecular masses of the two proteins as 17,746.3 and 15,699.9 [DnaBΔCs (162-470) and (143-470), respectively; *cf.* calculated masses of 17,744.7 and 15,700.6]. Although the N-terminal domain has been reported to exert a strong influence on hexamer formation in the native protein (11), sedimentation equilibrium studies on the two DnaB N-terminal fragments showed that both are monomeric. Plots of protein concentration versus radius (not shown) gave excellent fits to apparent molecular weights of 13,710 [DnaBΔC-

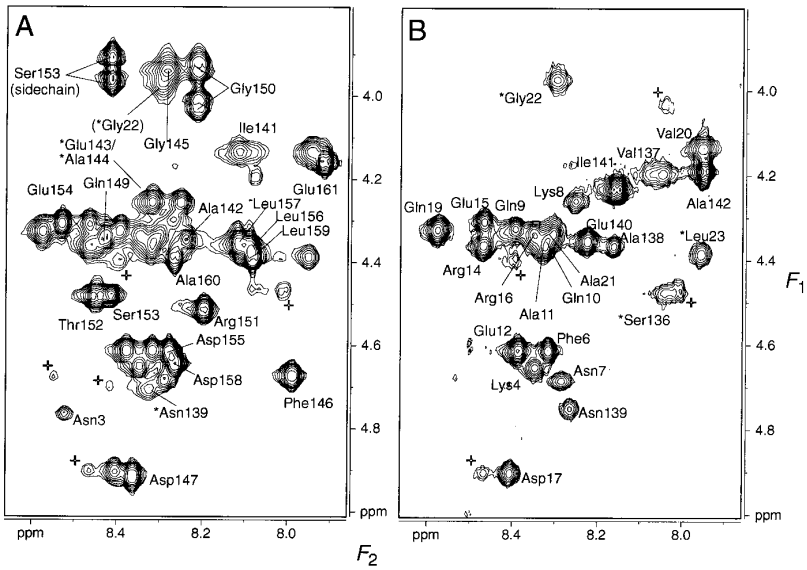

FIG. 2. TOCSY spectra of (A) DnaBΔC(162-470) and (B) DnaBΔC(143-470). The fingerprint region with the H^{α} -H^{N} cross peaks is shown. The cross peaks are labelled with their sequence specific assignments. Stars identify tentative assignments. Unassigned spin systems are marked with a cross.

(143-470), 1 mg/mL, Buffer E], 18,900 [DnaBΔC(162-470), 1 mg/mL, Buffer D] and 19,100 [DnaBΔC(162-470), 4 mg/mL, Buffer D].

Circular dichroism studies of DnaBΔC(162-470) were carried out to obtain secondary structure information and to probe the stability of the fragment at varying temperatures and pH. The protein was observed to be mostly α-helical and stable up to 35 °C and at pH values above 6.0. The protein denatured reversibly if the temperature was raised to 70 °C with a denaturation temperature of about 45 °C. Reversible denaturation was also observed at pH values below 5 at room temperature.

Initial NMR studies were carried out on DnaBΔC-(162-470). The spin systems of about 30 flexible amino acid residues could be identified in the TOCSY spectrum (Fig. 2A). The sequence-specific resonance assignments, however, were difficult to obtain because of extensive spectral overlap. At this stage, only resonances from residues 141-142 and 145-161 could be sequence-specifically assigned from the H^{α}-H^{N} connectivities in the F_1,F_2-doubly-decoupled ROESY spectrum.

In order to facilitate assignments by reducing spectral overlap, DnaBΔC(143-470) was constructed. This enabled the sequential resonance assignment of residues 4-21 and 137-142 from TOCSY, F_1-decoupled ROESY and conventional ROESY spectra. In total, the spin systems of 29 residues were identified in the TOCSY spectrum (Fig. 2B). The amide protons of the first three N-terminal residues exchanged too rapidly with the solvent to be observable. Yet, the signals of the non-exchangeable protons of Ala 1 could be assigned from TOCSY correlations, and the resonances of Asn 3 were assigned by comparison with the spectra of DnaBΔC(162-470), where the H^{N} resonance of Asn 3 was observed (Fig. 2A). For three more spin systems the TOCSY correlations were found but the sequential ROESY connectivities were too weak to be observed. These spin systems belong to a glycine, a leucine and a serine residue and presumably represent the residues between the flexible tails and the conformationally rigid core of the protein (Fig. 2B). The resonance assignments of DnaBΔC(143-470) confirmed those of DnaBΔC(162-470). The cross peaks assigned to residues 145-161 (Fig. 2A) are absent in the spectrum of the smaller fragment (Fig. 2B). In total, resonance assignments were obtained for residues 1-23 and 136-142 of DnaBΔC(143-470) and for residues 141-161 of DnaBΔC(162-470).

The chemical shifts of the assigned resonances of the non-exchangeable protons deviate insignificantly from tabulated random coil chemical shifts (30,31). For DnaBΔC(143-470), the only deviations larger than 0.1 ppm were measured for the sidechain H^{N} resonances of arginine residues 14 and 16, sidechain H^{γ} and H^{δ} resonances of proline residues 5, 13 and 18 and the H^{α} resonances of the terminal, charged amino acid residues. For DnaBΔC(162-470), deviations larger than 0.1 ppm were observed for the H^{α} resonances of Arg 151, Thr 152, Asp 156, Asp 159 and Glu 161, the H^{β} resonances of Thr 152 and Asp 159, and the H^{δ} resonances of Pro 148. The deviations occurred along the polypeptide chain in an apparently uncorrelated way, and were all but one smaller than 0.2 ppm. Consequently, the chemical shifts do not indicate any regular secondary structure for these segments. The tabulated

data from (30) have been used as a reference for all random coil data except for residues preceding proline residues, where values from Wishart *et al.* (31) were used. For the latter, the random coil data of (30) differ from those of (31) by about 0.3 ppm.

The mobility of the assigned residues in DnaBΔC-(143-470) was confirmed by their resonance linewidths in the F_1,F_2-doubly-decoupled TOCSY spectrum. The linewidths of amide proton resonances from the structured core of the protein were about 30 Hz as measured from a 1D ^{1}H NMR spectrum. The average linewidth of the amide proton resonances of residues 4-23 was 13 Hz, with a maximum value of 25 Hz for Asn 7 and a minimum value of 8 Hz for Glu 12. The amide proton resonance linewidths of residues 137-142 decrease towards the C-terminus from 16 to 5 Hz, with an average value of 11 Hz. The significantly decreased linewidths of the flexible ends illustrate their increased mobility on the nanosecond time scale. Notably, the H^{α}-H^{N} cross peaks observed for the flexible ends in the TOCSY spectrum of DnaBΔC(143-470) are all present in the corresponding spectrum of DnaBΔC(162-470). Only a few chemical shifts changed due to the slightly different pH used and the different carboxyl termini. The H^{α}-H^{N} cross peak of Asn 3 is visible in the spectrum of DnaBΔC(162-470) (Fig. 2A) but absent from the spectrum of DnaBΔC(143-470) (Fig. 2B), presumably because of the somewhat higher pH used. It is apparent that the presence of residues 143-161 does not increase the size of the structured core of the protein.

In conclusion, the present data show that the N-terminal domain of DnaB is an independent folding unit with a structurally well-defined, α-helical core comprising residues 24-136. Residues 1-23 and 137-161 are in random coil conformations and are mobile on a nanosecond time scale. The presence of a long, flexible linker region between the amino and carboxyl terminal domains of DnaB is further supported by proteolytic studies (3). The present accurate delineation of the structured part of the N-terminal domain of DnaB illustrates how NMR can be used to guide the construction of protein fragments which are more readily amenable to structural analysis by X-ray crystallography or NMR spectroscopy.

ACKNOWLEDGMENTS

Financial support from the Swedish Natural Science Research Council (Project 10161), the Wallenberg Foundation, and the Erik and Edith Fernström Foundation for Medical Research is gratefully acknowledged. We also thank Penny Lilley and Drs. Peter Jeffrey, Greg Kilby, and Denis Shaw of the Australian National University for technical assistance and for carrying out the sedimentation equilibrium, electrospray mass spectrometry, and N-terminal protein sequence analyses, respectively.

REFERENCES

1. Arai, K., and Kornberg, A. (1981) *J. Biol. Chem.* **256,** 5260–5266.
2. Bujalowski, W., Klonowska, M. M., and Jezewska, M. J. (1994) *J. Biol. Chem.* **269,** 31350–31358.
3. Nakayama, N., Naoko, A., Kaziro, Y., and Arai, K. (1984) *J. Biol. Chem.* **259,** 88–96.
4. Funnell, B. E., Baker, T. A., and Kornberg, A. (1987) *J. Biol. Chem.* **262,** 10327–10334.
5. Sekimizu, K., Bramhill, D., and Kornberg, A. (1988) *J. Biol. Chem.* **263,** 7124–7130.
6. Marszalek, J., and Kaguni, J. M. (1994) *J. Biol. Chem.* **269,** 4883–4890.
7. LeBowitz, J. H., and McMacken, R. (1986) *J. Biol. Chem.* **261,** 4738–4748.
8. Arai, K., and Kornberg, A. (1981) *J. Biol. Chem.* **256,** 5253–5259.
9. San Martin, M. C., Stamford, N. P. J., Dammerova, N., Dixon, N. E., and Carazo, J.-M. (1995) *J. Struct. Biol.* **114,** 167–176.
10. Yu, X., Jezewska, M. J., Bujalowski, W., and Egelman, E. H. (1996) *J. Mol. Biol.* **259,** 7–14.
11. Biswas, S. B., Chen, P.-H., and Biswas, E. E. (1994) *Biochemistry* **33,** 11307–11314.
12. Nakayama, N., Arai, N., Bond, M. W., Kaziro, Y., and Arai, K. (1984) *J. Biol. Chem.* **259,** 97–101.
13. Stamford, N. P. J. (1992) Ph.D. Thesis, Australian National University.
14. Elvin, C. M., Thompson, P. R., Argall, M. E., Hendry, P., Stamford, N. P. J., Lilley, P. E., and Dixon, N. E. (1990) *Gene* **87,** 123–126.
15. Love, C. A., Lilley, P. E., and Dixon, N. E. (1996) *Gene* **176,** 49–53.
16. Studier, F. W., Rosenberg, A. H., Dunn, J. J., and Dubendorff, J. W. (1990) *Methods Enzymol.* **185,** 60–89.
17. Bradford, M. M. (1976) *Anal. Biochem.* **72,** 248–254.
18. Briand, J., and Ernst, R. R. (1991) *Chem. Phys. Lett.* **185,** 276–285.
19. Bothner-By, A. A., Stephens, R. L., Lee, J.-M., Warren, C. D., and Jeanloz, R. W. (1984) *J. Am. Chem. Soc.* **106,** 811–813.
20. Kessler, H., Griesinger, C., Kerssebaum, R. Wagner, K., and Ernst, R. R. (1987) *J. Am. Chem. Soc.* **109,** 607–609.
21. Brüschweiler, R., Griesinger, C., SØrensen, O. W., and Ernst, R. R. (1988) *J. Magn. Reson.* **78,** 178–185.
22. Otting, G., Orbons, L. P. M., and Wüthrich, K. (1990) *J. Magn. Reson.* **89,** 423–430.
23. Hammarström, A., and Otting, G. (1994) *J. Am. Chem. Soc.* **116,** 8847–8848.
24. Geen, H., and Freeman, R. (1991) *J. Magn. Reson.* **93,** 93–141.
25. Weigelt, J., Hammarström, A., Bermel, W., and Otting, G. (1996) *J. Magn. Reson. B* **110,** 219–224.
26. Silver, M. S., Joseph, R. I., and Hoult, D. I. (1984) *J. Magn. Reson.* **59,** 347–351.
27. Ernst, R. R., Bodenhausen, G., and Wokaun, A. (1987) Principles of Nuclear Magnetic Resonance in One and Two Dimensions, Clarendon, Oxford.
28. Friedrichs, M. S. (1995) *J. Biomol. NMR* **5,** 147–153.
29. Güntert, P., Dötsch, V., Wider, G., and Wüthrich, K. (1992) *J. Biomol. NMR* **2,** 619–629.
30. Wüthrich, K. (1986) NMR of Proteins and Nucleic Acids, Wiley, New York.
31. Wishart, D. S., Bigam, C. G., Holm, A., Hodges, R. S., and Sykes, B. D. (1995) *J. Biomol. NMR* **5,** 67–81.